2014-01-1366

SI engine control in the cold-fast-idle period

for low HC emissions and fast catalyst light off

Author, co-author (Do NOT enter this information. It will be pulled from participant tab in MyTechZone)

Affiliation (Do NOT enter this information. It will be pulled from participant tab in MyTechZone)

ABSTRACT

The engine and its exhaust flow behaviors are investigated in a turbo-charged gasoline direct injection engine under simulated cold-fast-idle condition. The metrics of interest are the exhaust sensible and chemical enthalpy flows, and the exhaust temperature, all of which affect catalyst light off time. The exhaust sensible enthalpy flow is mainly a function of combustion phasing; the exhaust chemical enthalpy flow is mainly a function of equivalence ratio. High sensible and chemical enthalpy flow with acceptable engine stability could be obtained with retarded combustion and enrichment. When split injection is employed with one early and one later and smaller fuel pulse, combustion retards with early secondary injection in the compression stroke but advances with late secondary injection. Comparing gasoline to E85, the latter produces a lower exhaust temperature because of charge cooling effect and because of a faster combustion.

INTRODUCTION

Downsized turbocharged direct-injection spark ignition (DISI) engines can achieve superior fuel economy with the same or better performance [1]. However, compared to similar naturally aspirated engines, there are significant cold-start emission issues. The focus of this paper is on hydrocarbon (HC) emissions.

SI engine emission control relies on three-way catalyst technology. The catalyst, however, is ineffective when cold [2]. For fast catalyst warm-up, conventional strategies such as using close-coupled catalysts and exhaust manifolds with coatings and/or low thermal inertia are less effective when applied to turbo DISI engines. The warm-up of the catalyst is hindered by the heat transfer to the turbocharger assembly which is typically located upstream of the catalyst. Furthermore, emission rates of unburned hydrocarbons during cold-start are higher because of the presence of substantial in-cylinder liquid fuel due to direct fuel injection. Hence,

reducing the cumulative cold-start emissions of unburned hydrocarbons from a turbocharged DISI engine is more challenging than that in a naturally aspirated, port-fuel-injection (PFI) engine.

In this paper, the effects of fuel injection timing, split injection, ignition timing, and fuel ethanol content on the sensible and chemical enthalpy flow to the catalyst are characterized.

BACKGROUND

To improve cold-start performance, the metrics of interest are the exhaust sensible enthalpy flow, exhaust gas temperature, and exhaust chemical enthalpy flow. These metrics strongly influence catalyst warm-up time and exhaust emissions during warm-up.

In this research, combustion phasing is used to control exhaust sensible enthalpy flow and exhaust gas temperature; enrichment is used to stabilize combustion and to enhance chemical enthalpy flow for the potential benefit of secondary air injection; and split injection is used to locally enrich the in-cylinder mixture for combustion stability at retarded combustion phasing. Engine emissions with E85 fuel are also assessed.

Ignition timing

Late ignition timing is a common strategy for fast catalyst warm-up. Retarded combustion reduces work transfer from cylinder gases to the piston resulting in higher exhaust temperature. For constant engine torque, the reduced fuel conversion efficiency associated with late combustion requires greater fuel and air flow rate. Thus late ignition leads to greater engine-out sensible enthalpy flow due to both higher temperatures and greater mass flow rates. Late combustion is limited by increasing cycle-to-cycle variation. Very late

combustion could lead to partial-burn or incomplete combustion, resulting in unacceptable level of HC emissions.

Mixture enrichment

Rich mixtures are useful during cold start for two reasons. First, enrichment can improve combustion stability and reduce cycle-to-cycle combustion variations. Second, a strategy employing late ignition timing with rich mixtures and air injection to the exhaust manifold (i.e. secondary air injection) has been successful to simultaneously reduce feed-gas emissions and to accelerate catalyst warm-up [3]. This research does not experimentally investigate secondary air injection, but quantifies the chemical enthalpy flow rate which is proportional to the potential chemical heat release available when secondary air is used. Mixture enrichment has a potential drawback in terms of sensible enthalpy flow rate: rich mixtures lead to lower exhaust gas temperatures due to extra evaporative charge cooling and reduction in combustion efficiency.

Split fuel injection

Direct fuel injection affords the ability to have multiple injections per cycle. Split injection with an injection during the intake stroke, and a shorter injection late in the compression stroke can provide local enrichment near the spark plug to stabilize early combustion without global mixture enrichment. [4]. Split injection also diminishes fuel jet wall wetting, thereby reduces engine-out emissions. Adequate fuel pressure is required to provide sufficient atomization [1, 5]. There are concerns that late fuel injection could lead to excessive piston impingement and subsequent PM emissions due to the excessive liquid fuel presence on the combustion chamber surfaces.

Fuel ethanol content

Fuels containing significant ethanol content present an additional emissions challenge for turbocharged DISI engines. Ethanol has a substantially higher latent heat of vaporization than gasoline. The lower heating value of ethanol also requires a greater quantity of fuel to be injected for the same torque output. Both attributes would lead to significant charge cooling and hinders fuel vaporization, which, in turn, would worsen cold-start emissions.

EXPERIMENTAL SETUP

Engine experiments were carried out on a production GM 2.0L inline-4 16-valve turbocharged gasoline direct injection spark ignition engine (GM LNF series). The production engine as equipped with independent variable` cam phasing on the intake and exhaust camshafts. Table 1 -3 summarize the engine and valve specifications.

Table 1:Engin e specifications

Engine type	Inline 4 cylinder
Displacement [cc]	1998
Bore [mm]	86
Stroke [mm]	86
Wrist pin offset [mm]	0.8
Connecting rod [mm]	145.5
Compression ratio	9.2:1
Fuel system	Side-mounted, gasoline direct injection
Valve configuration	16 valve DOHC, dual cam phaser, 35.1 mm intake valve diameter, 30.1 mm exhaust valve diameter

Table 2: Intake valve timing and lift information.

Intake Valve	Opens [$ATDC_{gas\ ex}$]	Max open [$ATDC_{gas\ ex}$]	Closes [$ABDC_{compr}$]
Base	+11°	+126°	+61°
Max advance	-39°	+76°	+11°
Lift [mm]	0.25mm	10.3mm	0.25mm

Table 3: Exhaust valve timing and lift information.

Exhaust Valve	Opens [$BBDC_{exp}$]	Max open [$ATDC_{gas\ ex}$]	Closes [$ATDC_{gas\ ex}$]
Base	+52°	-125°	-10°
Max retard	+2°	-75°	+40°
Lift [mm]	0.25mm	10.3mm	0.25mm

The fuel used is a Haltermann HF0437 Tier II EEE certification fuel with RON of 96.5 and MON of 88.6. For E85 experiments, HF0437 is splash-blended on-site with anhydrous 99.9% pure ethanol by volume.

Engine control was accomplished using a custom desktop PC control system. The hardware allowed real time control of fuel injector pulse width, ignition timing, intake camshaft timing, exhaust camshaft timing. Fuel supply pressure was held constant by a hydraulic accumulator driven by high pressure nitrogen gas at 5 MPa.

Exhaust gas temperatures are measured in the manifold approximately 3 cm downstream of the flange. The thermocouple is equipped with a custom-built aspirated radiation shield to reduce error due to radiation and exhaust mass flow rate pulses during the exhaust process.

Hydrocarbons are measured with a Cambustion HFR400 Fast Flame Ionization Detector (FFID). Measurements are conducted at two points. The first is exhaust manifold runner of cylinder 4 (nearest the flywheel) approximately 6 cm

downstream of the flange. The second is downstream of the turbocharger outlet.

Carbon monoxide, and carbon dioxide are measured with a Horiba MEXA-554JU and a Horiba MEXA-584L. Samples are drawn through an ice-bath condenser and lab dessicant column from the exhaust manifold runner of cylinder 4. The dry measurements have been converted to wet values using the measured λ values.

Experimental conditions

The experiments have been conducted at a speed/load operating point meant to represent the quasi-steady fast-idle period that occurs after cranking and speed flare during cold start. The engine operating conditions used for these experiments are based on values representing typical fast idle condition in practice, and are summarized in Table 4.

Table 4- Nominal operating condition for quasi-steady fast idle portion of cold start.

Engine parameter	Value	Units
Engine speed	1200	rpm
NIMEP	2.0	bar
Ignition	Varied	CAD ATDC
Fuel/air equivalence ratio (Φ)	1	-
External EGR	0	%
Coolant/oil temperature	20	°C
Fuel inj.timing	80	CAD ATDC$_{gas ex}$
Fuel inj. pressure	5.0	MPa
Intake air temperature	20	°C
Exhaust back pressure	5	kPa

Except the split injection experiments, experiments use single pulse fuel injection per cycle. All experiments used valve timing in the park position.

RESULTS

Exhaust sensible enthalpy flow

When ignition timing is retarded from 7 CAD BTDC to 17 CAD ATDC, the 50% mass-fraction-burn (m.f.b.) crank angle (denoted by CA50) shifts from 36° to 84° ATDC. The exhaust gas temperature varies almost linearly from 525K to 750K. Figure 1 shows exhaust sensible enthalpy flow (referenced to 298K) increases from appoximately 4.2 kW to 11.5kW over this range of combustion phasing which is characterized by the CA50 values. The variation is super-linear because NIMEP is held constant. Then more fuel and air are required as combusiton is retarded because of the assocated decrease in indicated fuel conversion efficiency.
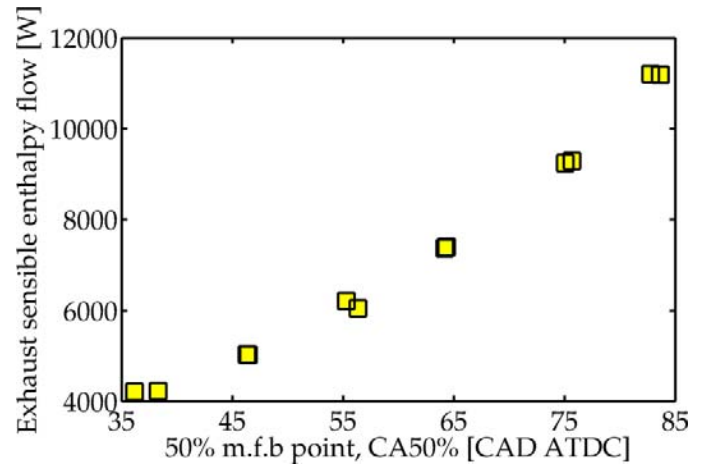
Figure1: Exhaust thermal enthalpy flow increases from 4.2kW to 11.5kW while NIMEP and mixture stoichiometry are held constant as CA50 changes from 36° to 84° ATDC.

Retarded combustion leads to higher sensible enthalpy flow, but also to larger cycle-to-cycle variability; see Fig. 2. At COV of GIMEP greater than approximately 10%, misfire was sometimes observed as short-lived lean spikes on the lambda sensor signal.
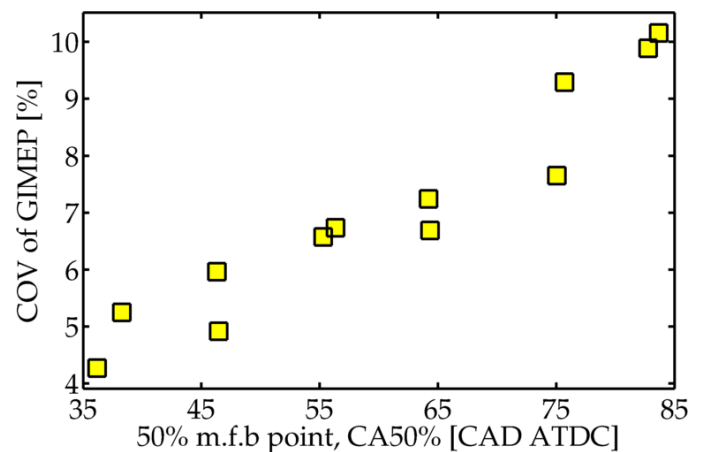

Figure 2: COV of GIMEP as a function of combustion phasing as indicated by the CA50 values.

For robust combustion at this cold-start fast-idle point, a maximum COV of GIMEP of 10% may be imposed. Then a maximum sensible enthalpy flow of 11.5 kW is readily achievable. This value is shown in the next section to be comparable to the chemical enthalpy flow achievable with mixture enrichment.

Exhaust chemical enthalpy Flow

The exhaust chemical enthalpy flow is the sum of the chemical enthalpy flow of the exhaust species of incomplete combustion. For each species, that value is the product of the individual mass flow rate and lower heating value. The components considered are CO, unburned hydrocarbons and

hydrogen. The hydrogen concentration is not measured directly, but is estimated using an empirical relationship based on the water gas shift equation with an equilibrium constant of K=3.5.

The contour map of the exhaust chemical enthalpy flow is shown in Fig. 3. At constant CA50 (along a vertical line in the figure), the chemical enthalpy flow increases almost linearly with increasing enrichment. The values increase more rapidly at later than at earlier combustion phasing because for the former, the air and fuel flow rates are higher so as to maintain constant NIMEP with the lower fuel conversion efficiency.
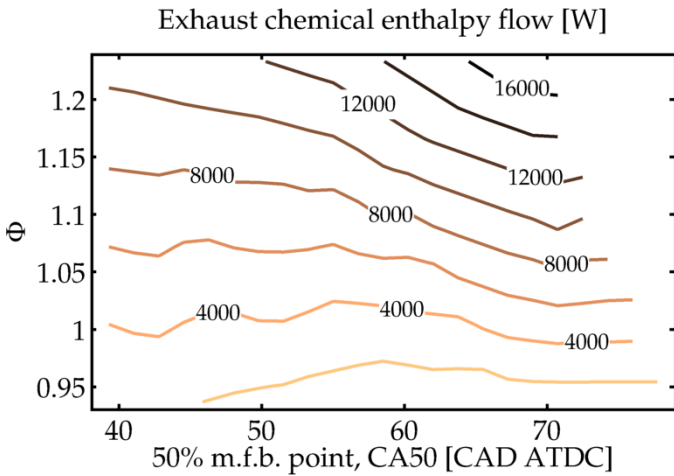
Figure 3: Exhaust chemical enthalpy flow increases with mixture enrichment, more steeply at later ignition timing when fuel flow rate is higher to maintain constant NIMEP.

The COV of GIMEP as a function of spark timing and fuel equivalence ratio is shown in Fig. 4. It is observed that enrichment from stoichiometric reduces the COV for CA50 values up to 70° ATDC in the experiment. At $\Phi = 1.2$, the COV is less than 10% when CA50 is 70 CAD ATDC.

The exhaust temperature as a function of CA50 is shown in Fig. 5. The temperature is most sensitive to combustion phasing, and does not decrease significantly with mixture enrichment.

The combined (sensible + chemical) enthalpy flow for the feed gas as a function of Φ and CA 50 is shown in Fig. 6. Comparing the value at CA50 of 40 CAD ATDC and $\Phi = 1.0$ to that at CA50 of 65 CAD ATDC and $\Phi = 1.25$, the rich mixture with late combustion offers stable combustion and a potential increase to total enthalpy flow of more than 300%.
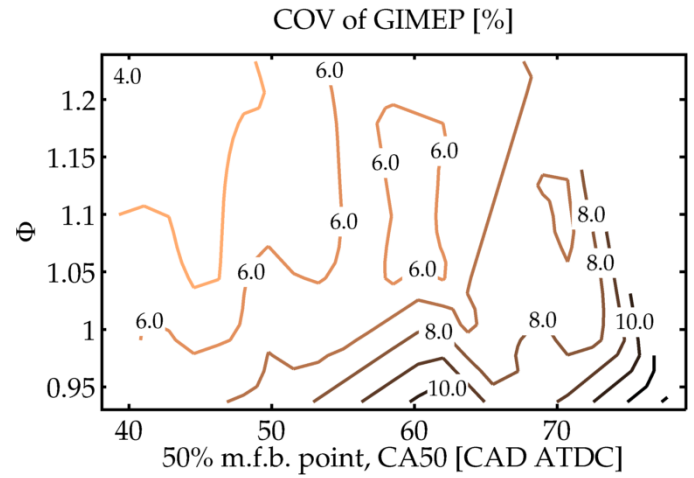

Figure 4: Rich mixtures have good combustion stability (low COV) even for late ignition.
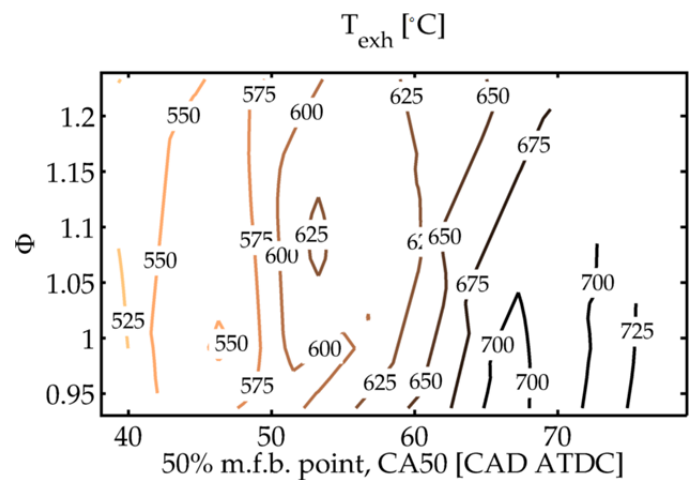

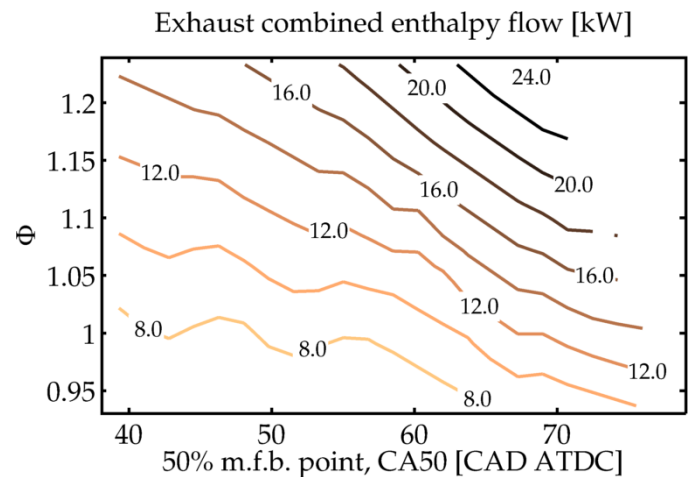Figure 5: Exhaust gas temperature as a function of Φ and CA50.

Figure 6: Combined (sensible + chemical) enthalpy flow as a function of Φ and CA50.

The flow rate of unburned HC in the exhaust is shown in Fig. 7. When Φ reaches 1.25, HC increases by approximately

350% compared to the values at stoichiometric. Thus using enrichment as a strategy for combustion stability is only justifiable if secondary air injection is successfully used to reduce the feed gas emissions before they enter the cold, inactive catalyst.
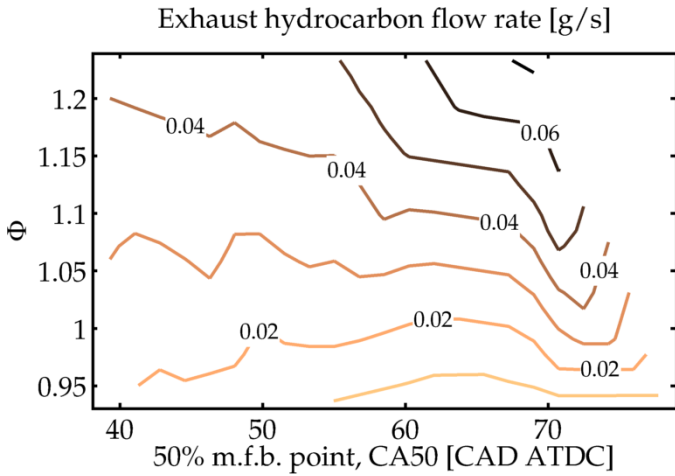

Figure 7: The mass flow rate of unburned hydrocarbons as a function of Φ and C A50.

Split injection experiments

Normally fuel is delivered as one single injection pulse during the early intake stroke to have sufficient time for complete mixing and evaporation. A split injection strategy delivers the majority of fuel during the intake stroke, with a second smaller injection late in the compression stroke. The fuel from the second pulse is not fully mixed with the charge, and it creates, near the spark plug, a locally rich mixture which could enhance early flame development and stabilize combustion, especially for significantly retarded ignition.

Figure 8 shows the piston and injector from the engine used in this research. The piston features specialized crown geometry to enhance the stratification effect. A 70/30 (by fuel volume) split is used. The choice is limited by the lower bound for consistent injection duration of the second pulse.

In order to examine any interaction with, or variation resulting from piston motion effects, sweeps of second injection timing were performed at three different ignition timing. The start of the second injection, late in the compression stroke is referred to as SOI2. The first injection started at 60 CAD ATDC-intake. The overall fuel equivalence ratio is stoichiometric ($\Phi = 1$) for these experiments.

Figure 8: The engine used in this research uses injector targeting and piston crown bowl geometry to enhance mixture preparation during cold start.

The effect of SOI2 on engine stability is shown in Fig. 9. Early secondary injection (in the intake stroke) is similar to a single injection in terms of mixing, and the COV of GIMEP is not sensitive to the timing. For all the three spark timings, the COV values, however, increases with SOI2 retard in the compression stroke until 290 CAD ATDC-intake. This increase have to do with that when the charge is stratified, the leaner part of the charge may reach the spark plug at ignition, and adversely affect the flame development process. When SOI2 goes beyond 290 CAD ATDC-intake, the richer mixture may then reach the spark plug at ignition; the COV values begin to decrease. For the whole range of SOI2 tested, however, the COV values are comparable to or larger than the single injection value.

It should be pointed out that while the overall feature of the above observation may be general, the quantitative details depend on the mixing and transport processes of the fuel vapor. Thus the phenomenon is engine and calibration specific.
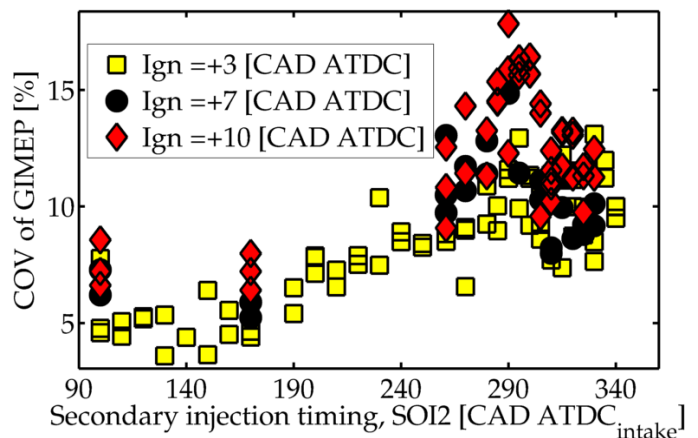

Figure 9: COV of GIMEP as a function of secondary injection timing; spark at 3, 7 and 10 CA degree ATDC-compression respectively.

The corresponding CA50 and 10% to 90% burn duration are shown in Figures 10 and 11. The behaviors of these values as a function of SOI2 are consistent with the above description.
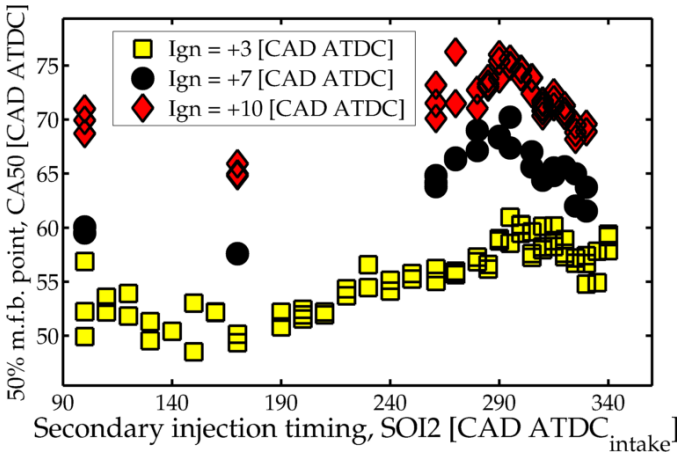

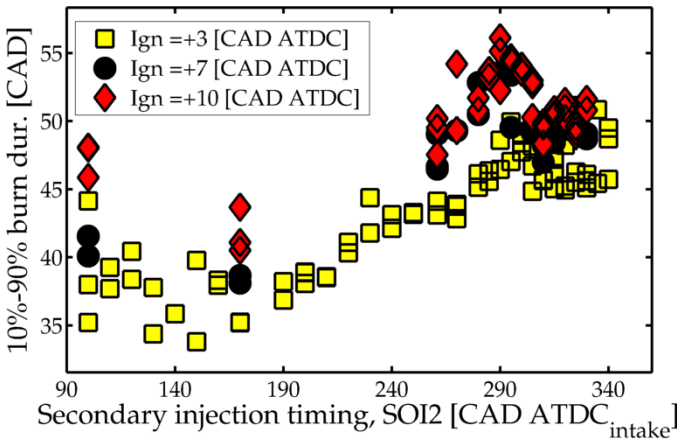Figure 10: CA50 as a function of SOI2.

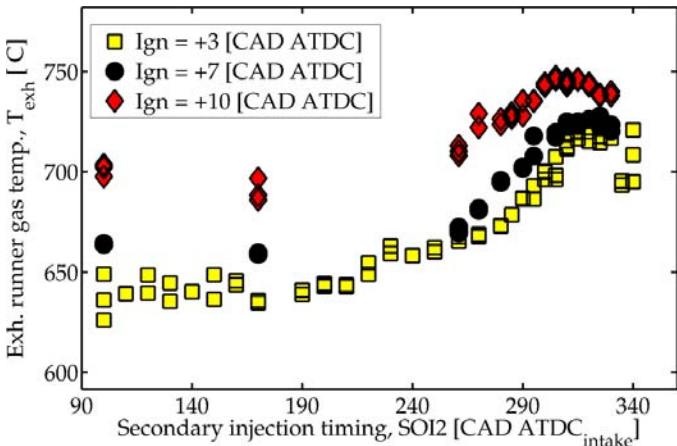Figure 11: Burn duration (10% to 90% m.f.b) as a function of SOI2.

Figure12: Exhaust gas temperature as a function of SOI2.

The exhaust gas temperature as a function of SOI2 is shown in Fig. 12. The values depend on the combustion phasing: later combustion gives a higher exhaust temperature as less work is extracted by the piston.

The exhaust HC as a function of SOI2 is shown in Fig. 13. The values drop substantially at when SOI2 is later than 240 CAD ATDC-intake. The exhaust temperature also rises substantially in this region. The drop in HC is attributed to the increase in post-flame oxidation of the crevice HC [6] due to the higher temperature in the expansion process as a result of the retarded combustion.

An additional factor is that split injection results in a mixture distribution that is rich near the center, in the mixture that burns first. The last regions to burn, and the gas stored in piston ring crevices at the perimeter of the combustion chamber is comparatively lean. Hence post-flame oxidation may be enhanced by greater oxygen availability late in the expansion stroke.
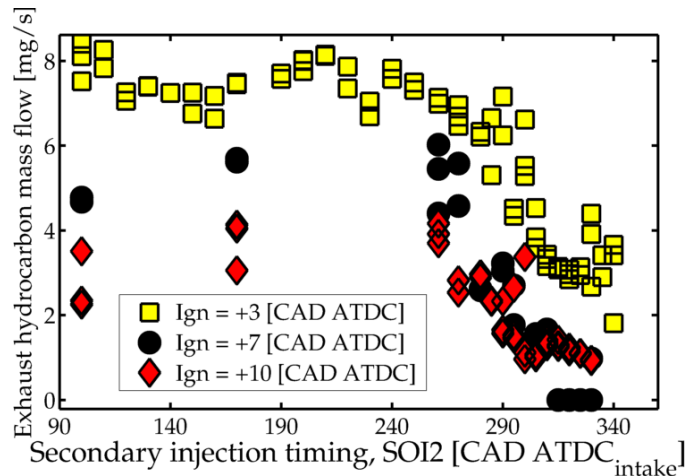

Figure 13: Unburned HC flow as a function of SOI2.

The exhaust sensible enthalpy flow is shown in Fig. 14. The value increases with retard of SOI2 because of the increase in exhaust temperature associated with retard combustion.

The exhaust chemical enthalpy flow is shown in Fig. 15. The drop in values when SOI2 is retarded beyond 240 CAD ATDC-intake is attributed to the decrease in HC emissions because of post-flame oxidation at the higher expansion charge temperature.

Figure 9 shows that split injection does not improve stability compared to single injection. Stability improvement has been observed in prior work done on split injection [4] with very late injection. (In [4], secondary injection took place in the expansion stroke overlapping with the spark event. In our experiment, the engine would not operate reliably at such late injection.) The engine response to secondary injection depends on the details of the spray geometry with respect to the combustion chamber and spark plug.
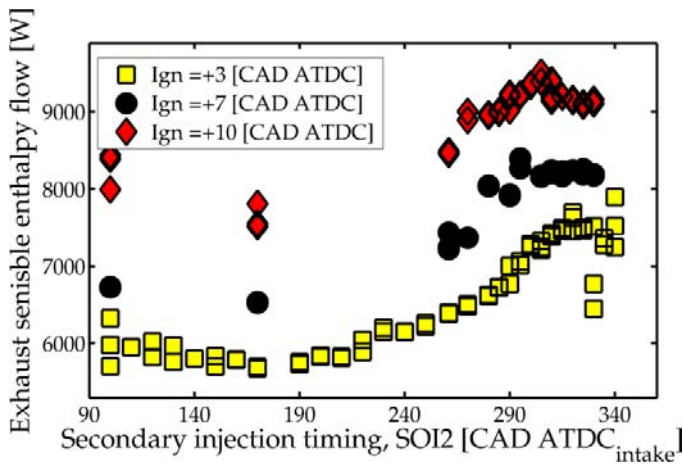
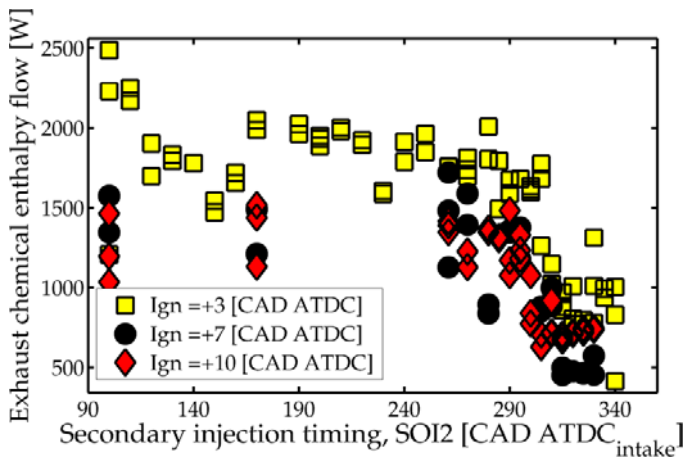Figure 14: Exhaust sensible enthalpy flow as a function of SOI2.

Figure15: Exhaust chemical enthalpy flow as a function of SOI2.

E85 experiments

The exhaust from engines fueled with E85 contains oxygenate species such as the ethanol and aldehydes. The flame ionization detector (FID) used for HC emissions measurement has reduced sensitivity to oxygenated species. A correction to the FID signal based on the method described in [7] is used to obtain the concentration of carbon in the exhaust organic gases. To obtain the mass flow rate of the organic gas, the organic gas is assumed to have the same hydrogen to carbon and oxygen to carbon ratios as the fuel.

The organic gas emissions as a function of SOI2 are shown in Fig. 16. The values are higher for E85 than for E0 (neat gasoline). There are several factors which affects the organic gas emissions in using E85:

1. Because of the lower heating value of E85 (29.3 MJ/kg versus 44 MJ/kg for E0), more fuel has to be injected for the same NIMEP. (If all other factors are kept equal, the fuel mass ratio is 44/29.3=1.5) Thus there is more in-cylinder liquid fuel which contributes to the higher emission.

2. The heating values per unit mass of the stoichiometric mixture of E0 and E85 are about the same (2.83 versus 2.72 MJ/kg; the LHV of E85 is lower, but the stoichiometric A/F is lower), therefore the trapped masses are about the same. The peak pressure for E85 is lower because the specific heats for both the unburned and burned gases are higher. Therefore, the trapped crevice mass is lower for the E85 case.
3. Because the stoichiometric A/F ratio is much lower for E85 than E0 (9.8 versus 14.6), the mass fraction of organic gas in the trapped crevice mass is higher (excluding residual gas, it is 9.3% versus 6.4%).

The factors 1 and 3 dominate over factor2. Thus the organic gas emissions are higher for E85 compared to E0 as fuel.
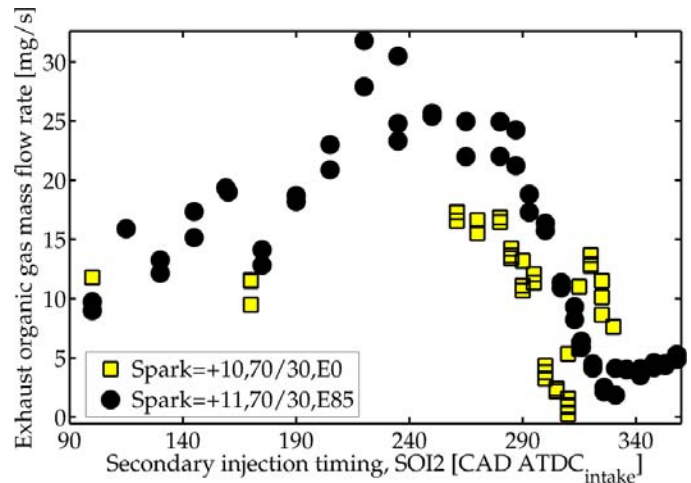

Figure16: Exhaust organic gas flow versus SOI2 for E0 and E85 fuels at NIMEP=2 bar. The values in the legend are spark timing (ATDC), injection split, and fuel type.

At approximately the same spark timing (10 and 11 CAD ATDC) and at the same NIMEP, the exhaust temperature using E85 is approximately 40 to 60° C lower; see Fig. 17. This observation may be attributed to the following:

1. For E85, both the latent heat of vaporization and the mass of fuel injected are much larger than those of E0. There is substantial fuel cooling of the charge.
2. Combustion is faster with E85 because of the higher laminar flame speed. At the same spark timing, the CA50 values for E85 are approximately 5 to 9 CAD more advanced than that for E0; see Fig. 18. Thus more work is extracted in the E85 case and the exhaust temperature is correspondingly lower.
3. The specific heats of both the unburned and burned gas for E85 combustion are higher, thus the burned gas temperature is lower.
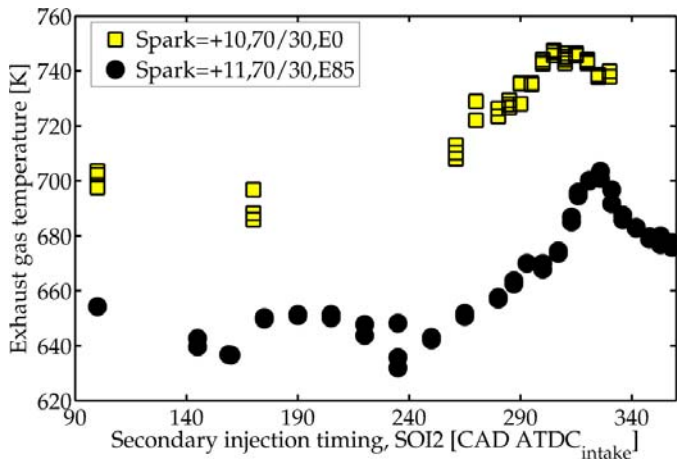
Figure 17: Exhaust temperature as a function of SOI2 for E0 and E85 fuels at NIMEP = 2 bar.
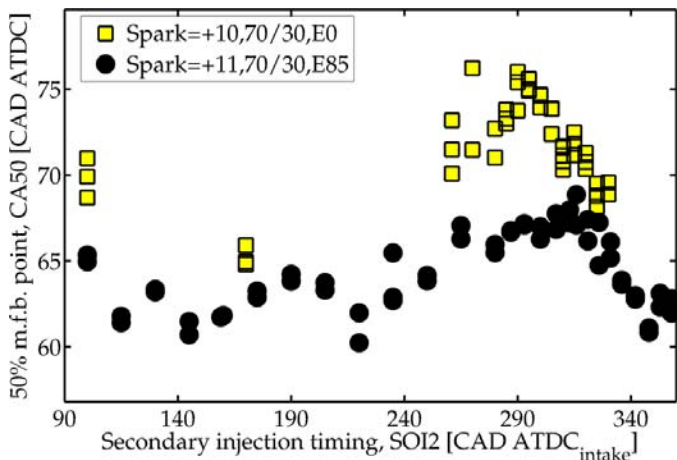

Figure18: CA50 versus SOI2 for E0 and E85 fuels at NIMEP = 2 bar.

SUMMARY/CONCLUSIONS

The effects of combustion phasing, enrichment, split injection and E85 versus E0 as fuel on the engine behavior at simulated cold-fast-idle condition have been assessed. The metrics are the combustion stability, exhaust gas temperature, exhaust sensible and chemical enthalpy flow, and exhaust HC flow.

The following conclusions are drawn:

1. The exhaust sensible enthalpy flow is primarily determined by combustion phasing.
2. The exhaust chemical enthalpy flow is primarily determined by the equivalence ratio. At constant NIMEP, it also increases with retarded combustion phasing because a higher throughput is then required to compensate for the reduced in fuel conversion efficiency.
3. The COV of GIMEP increases with combustion retard and decreases with enrichment from stoichiometric. At Φ =1.2, the COV is less than 10% at CA50 up to 70° ATDC.
4. Combination of enrichment and combustion retard provides a high engine-out total (sensible plus chemical)

enthalpy flow that could facilitate catalyst light off while keeping the COV of GIMEP at acceptable level. However, secondary air injection is necessary to burn off the products of incomplete combustion.

5. Split injection strategy has been assessed using a larger early injection (during intake) and a smaller late injection (during compression). As the secondary injection timing retards in the compression stroke, the CA50 first retards and then advances. The behavior is attributed to the local Φ value at the spark plug at ignition for the stratified charge. The exhaust temperature changes according to the combustion phasing.
6. At the same NIMEP, the organic gas emissions are higher for E85 than E0 because there is more liquid fuel in the cylinder, and that the crevice gas has a higher mass fraction of fuel because the stoichiometric A/F ratio for E85 is lower than that for E0.
7. The exhaust temperature for E85 is lower than that for E0 because there is more evaporative cooling of the burned gas, the specific heats of both unburned and burned gas are higher, and, when compared at the same spark timing, the combustion is faster.

REFERENCES

1. Davis, R., Mandrusiak, G., and Landenfeld, T., "Development of the Combustion System for General Motors' 3.6L DOHC 4V V6 Engine with Direct Injection," SAE Int. J. Engines 1(1):85-100, 2009, doi:10.4271/2008-01-0132.
2. *Technologies for Near-Zero-Emission Gasoline-Powered Vehicles*, Ed. F. Zhao, SAE International, Warrendale, PA, 2007.
3. Borland, M. and Zhao, F., "Application of Secondary Air Injection for Simultaneously Reducing Converter-In Emissions and Improving Catalyst Light-Off Performance," SAE Technical Paper 2002-01-2803, 2002, doi:10.4271/2002-01-2803.
4. Chen, X., Fu, H., Smith, S., and Sandford, M., "Investigation of Combustion Robustness in Catalyst Heating Operation on a Spray Guided DISI Engine," SAE Technical Paper, 2009-01-1489, 2009, doi:10.4271/2009-01-1489.
5. Gottschalk, W., Kirstein, G., Magnor, O., Schultalbers, M., et al., "Investigations on a Catalyst Heating Strategy by Variable Valve Train for SI Engines," SAE Technical Paper, 2012-01-1142, 2012, doi:10.4271/2012-01-1142.
6. Cheng, W., Hamrin, D., Heywood, J., Hochgreb, S. et al., "An Overview of Hydrocarbon Emissions Mechanisms in Spark-Ignition Engines," SAE Technical Paper 932708, 1993, doi:10.4271/932708.
7. Kar, K., and Cheng, W. "Using mass spectrometry to detect ethanol and acetaldehyde emissions from a direct injection spark ignition engine operating on Ethanol/Gasoline blends,", SAE Technical Paper, 2011-01-1159, 2011, doi:10.4271/2011-01-1159

CONTACT INFORMATION

Professor Wai Cheng, MIT, Bldg 31-165, 77 Massachusetts Avenue, Cambridge MA 02139. Email: wkcheng@mit.edu.

ACKNOWLEDGMENTS

DEFINITIONS/ABBREVIATIONS

A/F   Air fuel ratio

ATDC   After top-dead-center

BBDC   Before bottom-dead-center

CA50   Crank angle at 50% burn mass fraction

CAD   Crank angle degrees

COV   Coefficient of variation

DISI   Direct injection spark ignition

FID   Flame ionization detector

FFID   Fast-response flame ionization detector

GIMEP   Gross indicated mean effective pressure

HC   Hydrocarbon

LHV   Lower heating value

m.f.b.   Mass fraction burned

NIMEP   Net indicated mean effective pressure

PFI   Port fuel injection

PM   Particulate matter

SOI2   Start of secondary injection

Φ Fuel equivalence ratio

λ Air equivalence ratio